



## OPEN

## A supramolecular approach to fabricate highly emissive smart materials

## SUBJECT AREAS:

COLLOIDS

NANOPARTICLES

PREDICTIVE MARKERS

SELF-ASSEMBLY

Kai Liu<sup>1</sup>, Yuxing Yao<sup>1</sup>, Yuetong Kang<sup>1</sup>, Yu Liu<sup>2</sup>, Yuchun Han<sup>2</sup>, Yilin Wang<sup>2</sup>, Zhibo Li<sup>2</sup> & Xi Zhang<sup>1</sup><sup>1</sup>Key Lab of Organic Optoelectronics and Molecular Engineering, Department of Chemistry, Tsinghua University, Beijing 100084, China, <sup>2</sup>Institute of Chemistry, Chinese Academy of Sciences, Beijing 100190, China.Received  
27 March 2013Accepted  
22 July 2013Published  
6 August 2013Correspondence and  
requests for materials  
should be addressed to  
X.Z. (xi@mail.  
tsinghua.edu.cn)

The aromatic chromophores, for example, perylene diimides (PDIs) are well known for their desirable absorption and emission properties. However, their stacking nature hinders the exploitation of these properties and further applications. To fabricate emissive aggregates or solid-state materials, it has been common practice to decrease the degree of stacking of PDIs by incorporating substituents into the parent aromatic ring. However, such practice often involves difficult organic synthesis with multiple steps. A supramolecular approach is established here to fabricate highly fluorescent and responsive soft materials, which has greatly decreases the number of required synthetic steps and also allows for a system with switchable photophysical properties. The highly fluorescent smart material exhibits great adaptivity and can be used as a supramolecular sensor for the rapid detection of spermine with high sensitivity and selectivity, which is crucial for the early diagnosis of malignant tumors.

The aromatic chromophores, for example, perylene diimides (PDI), are well known for their desirable absorption and emission properties<sup>1–10</sup>. However, their stacking nature can lead to severely quenched emission<sup>11–16</sup>, which has greatly hindered the exploitation of their properties and further applications. To fabricate emissive aggregates or solid-state materials, it has been common practice to weaken the  $\pi$ - $\pi$  interactions of aromatic chromophores by the covalent attachment of substituents, e. g., bulky dendrons, into the aromatic rings, and it is quite efficient to fabricate highly fluorescent materials<sup>17–23</sup>, which, however, often involves difficult organic synthesis with multiple steps. Recently, aggregation-induced emission has been proven to be another efficient way to fabricate functional aggregates with high fluorescence<sup>24</sup>. However, only a limited number of chromophores exhibit this special property.

Besides the covalent methods mentioned above, we wonder if there is a supramolecular approach to suppress fluorescence quenching and to fabricate fluorescent and adaptive soft materials. Cucurbit[n]uril (CB[n]), a family of pumpkin-shaped macrocyclic hosts, has been developed into an interesting research area, because of their rich host-guest chemistry<sup>25–32</sup>. The CB[n] molecules are hydrophilic at their exterior, whereas it is hydrophobic inside their cavities. Because of the existence of the hydrophobic cavity, CB[n] has been widely used to encapsulate and solubilize dyes<sup>29–32</sup>, to enhance weak supramolecular interactions<sup>33,34</sup> etc. Herein, the large molecular volume and hydrophilic exterior of CB[n] molecules have encouraged us to explore the possibility of utilizing CB[n] as the bulky “noncovalent building blocks” to suppress the close stacking of chromophores in water, so as to obtain highly fluorescent materials. Moreover, the rich host-guest chemistry of CB[n] can enable the bulky substituents to be noncovalently and reversibly attached to the PDI aromatic rings, which can greatly decrease the number of required synthetic steps and also allows for a system with switchable photophysical properties.

For this purpose, a new kind of “dumbbell-shape” supramolecular amphiphile (supra-amphiphile) has been designed as shown in Figure 1. Supra-amphiphiles refer to amphiphiles that are formed on the basis of noncovalent interactions<sup>35–39</sup>. The advantages of supra-amphiphiles relate to their noncovalently synthesized nature, so the time-consuming covalent synthesis and purification process can be avoided to some extent. Here, perylene diimide (PDI), a remarkably photostable and highly fluorescent organic dye, is incorporated into one of the building blocks of the supra-amphiphile, Bola-form perylene diimide amphiphile (BPDI), acting as the rigid core. The other building block, CB[7], is selected as the bulky hydrophilic heads of the supra-amphiphiles. The strong host-guest interaction between CB[7] and naphthalene-methanaminium moiety<sup>40</sup> on BPDI is used as the driving force for the construction of the supra-amphiphile. It is anticipated that the “dumbbell-shape” supra-amphiphile can self-assemble into well-defined nanostructures in water owing to their amphiphilic nature, with the bulky CB[7] heads of the supra-amphiphile acting to weaken the  $\pi$ - $\pi$  interactions, thus preventing the fluorescence quenching of the PDI chromophores in the assemblies. Furthermore, the noncovalently prepared fluorescent soft materials may exhibit some adaptivity, inherited from the reversibility of the host-guest interaction, allowing the

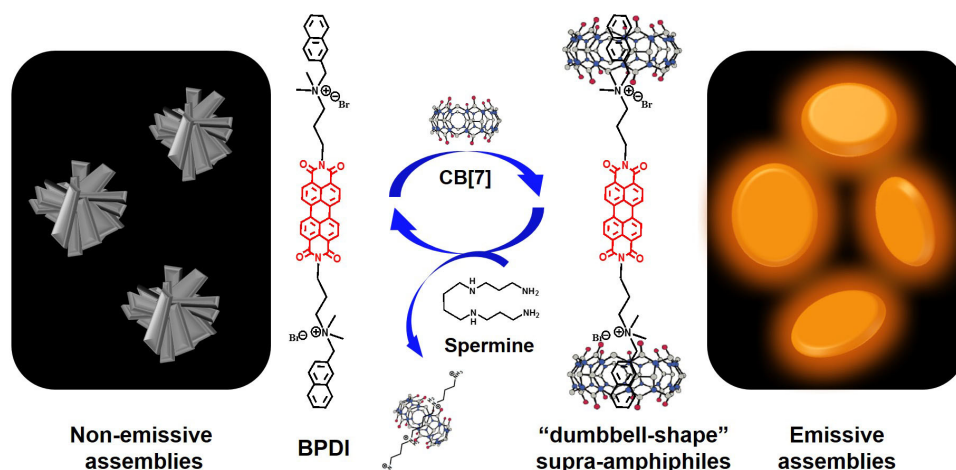


**Figure 1** | Schematic illustration of the fabrication of the adaptive “dumbbell-shape” supra-amphiphiles. PDI is incorporated into one of the building blocks of the supra-amphiphile, BPDl, acting as the rigid core. The other building block, CB[7], is selected as the bulky hydrophilic heads of the supra-amphiphiles. The strong host-guest interaction between CB[7] and naphthalene-methanaminium moiety on BPDl is used as the driving force for the construction of the supra-amphiphile. It is anticipated that the bulky CB[7] heads of the supra-amphiphile may suppress the fluorescence quenching of the PDI chromophores in the assemblies. Furthermore, the reversibility of the host-guest interaction may allow the supramolecular material to be used as a smart supramolecular sensor for spermine, an important tumor biomarker.

supramolecular material to be used as a smart supramolecular sensor for spermine, an important tumor biomarker.

## Results

**“Dumbbell-shape” supra-amphiphiles can be easily fabricated by mixing CB[7] with BPDl.** For the construction of the desired “dumbbell-shape” supra-amphiphiles, CB[7] and BPDl were mixed in water at a 2:1 molar ratio. Several observations and measurements support the hypothesis that supra-amphiphiles are formed. Firstly, the colors of the BPDl solution changed from orange to deep red after the addition of CB[7] (Figure 2a). The color change suggests that the packing arrangements of PDI chromophores in the assemblies have changed on the addition of

CB[7], resulting in a different electronic coupling of the  $\pi$ -systems. Secondly, from isothermal titration calorimetry results shown in Figure 2b, an abrupt transition point appears when the molar ratio of BPDl:CB[7] reaches 1:2, indicating the formation of BPDl/(CB[7])<sub>2</sub> supra-amphiphiles. The binding constant of naphthalene-methanaminium subgroup with CB[7] is calculated to be  $K = 4.4 \times 10^5 \text{ M}^{-1}$ . Thirdly, in mass spectroscopy (see Supplementary Figure S1), the peak at  $m/z = 1584.66$ , which corresponds to the complex of BPDl<sup>2+</sup>/(CB[7])<sub>2</sub>, was observed, further confirming the formation of BPDl/(CB[7])<sub>2</sub> supra-amphiphiles. Fourthly, as indicated by dynamic light scattering (DLS) measurements (Figure 2c), BPDl assemblies disappeared completely after the addition of CB[7]. Instead, smaller assemblies with a hydrodynamic diameter of

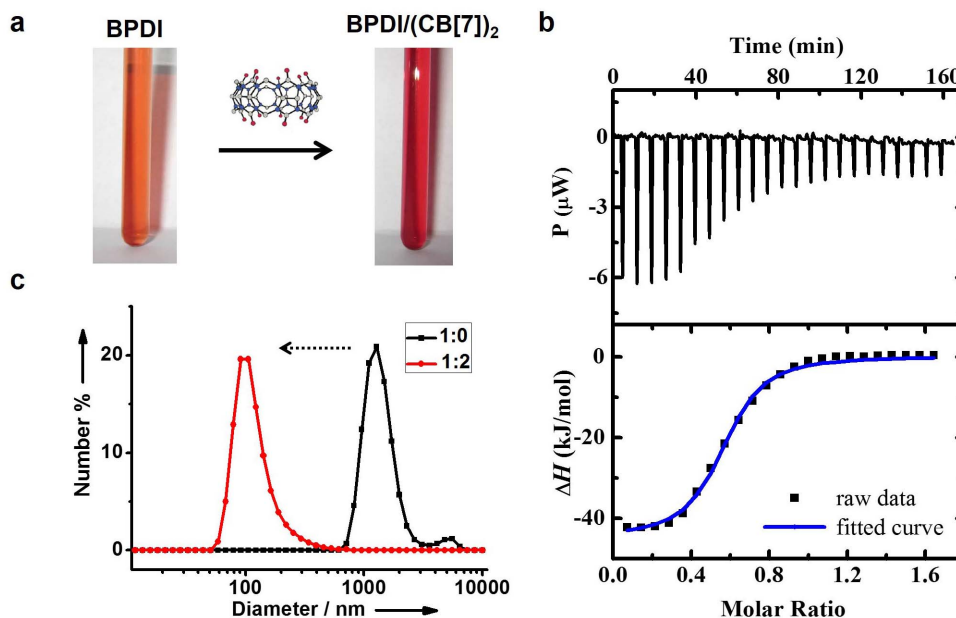


**Figure 2** | “Dumbbell-shape” supra-amphiphiles can be easily fabricated by mixing CB[7] with BPDl. (a) Photographs of the BPDl and the BPDl/(CB[7])<sub>2</sub> aqueous solutions. (b) ITC data for the titration of CB[7] with BPDl, “molar ratio” is defined as BPDl:CB[7]. (c) DLS measurements of the BPDl and the BPDl/(CB[7])<sub>2</sub> aqueous solution. The ratio in the inset of (c) is defined as BPDl:CB[7]. The concentration of BPDl is fixed at  $5.0 \times 10^{-4} \text{ M}$ .



~100 nm can be detected, indicating that the BPDI/(CB[7])<sub>2</sub> supra-amphiphiles show quite different self-assembling behavior compared with that of their building blocks.

**BPDI/(CB[7])<sub>2</sub> “dumbbell-shape” supra-amphiphiles self assemble into nanodiscs.** Electron microscopy indicated that the BPDI/(CB[7])<sub>2</sub> “dumbbell-shape” supra-amphiphiles self-assemble into nanodiscs in aqueous solution. The scanning electron microscope (SEM) image in Figure 3a clearly shows that nanodiscs with a diameter of ~400 nm. The thickness of the nanodiscs is measured to be several tens of nanometers from the side view images (see Supplementary Figure S2). To confirm that the formation of the nanodiscs is not related to the evaporation of the solvent during the vacuum condition in SEM, we conducted observations by cryogenic transmission electron microscope (cryo-TEM), as shown in Figure 3b. The cryo-TEM images of the nanodiscs are very similar to the SEM image, indicating that the nanodiscs are formed by self-assembly of the supra-amphiphiles in aqueous solution.

**BPDI/(CB[7])<sub>2</sub> “dumbbell-shape” supra-amphiphiles are efficient for the fabrication of highly fluorescent assemblies.** An interesting finding is that the fluorescence of the nanodiscs assembled by the “dumbbell-shape” supra-amphiphiles is greatly enhanced compared with the BPDI assemblies. As shown in Figure 4, in the BPDI assemblies, the fluorescence of the PDI chromophores is severely quenched. The quenching behavior should be ascribed to the “H-aggregated” nature of the PDI chromophores<sup>11,41</sup>, as indicated by the hypsochromic shift of absorption maxima (see Supplementary Figure S3). However, upon the addition of CB[7] into the aqueous BPDI solution, a dramatic increase of the fluorescence intensity at 570–750 nm is clearly observed. The emission intensity at 610 nm of BPDI/(CB[7])<sub>2</sub> supra-amphiphiles is about 100 times higher than that of BPDI, and the solution of the supra-amphiphiles becomes highly fluorescent, as shown in the inset of Figure 4 (see Section 6 in the Supplementary Information for detailed discussions).

In the nanodiscs assembled from the “dumbbell-shape” supra-amphiphiles, the close  $\pi$ - $\pi$  stacking of the core-located PDI chromophores may be weakened due to the influence of two bulky heads on the supra-amphiphiles, which can suppress the electronic coupling of the PDI aromatic rings in the “H-aggregates” thus leading to the enhanced fluorescence. We employed ultraviolet–visible spectroscopy (UV/Vis) and <sup>1</sup>H-nuclear magnetic resonance spectroscopy (<sup>1</sup>H-NMR) to illustrate this point. As shown in Figure 5a, as the ratio of CB[7]:BPDI increases, the absorption intensities increase gradually, whereas the PDI chromophores still remain in the “H-aggregated” state, as indicated by the unchanged pattern of the absorption bands. It has been well studied that the extent of hypochromism, i.e., the decrease in the molar extinction coefficient of the chromophores, is dependent on the distance and relative orientation between the chromophores<sup>42,43</sup>. Considering that no new absorption bands appear during the complexation process, the change of orientations of the PDI chromophores in the assemblies may be negligible<sup>11,20,44,45</sup>.

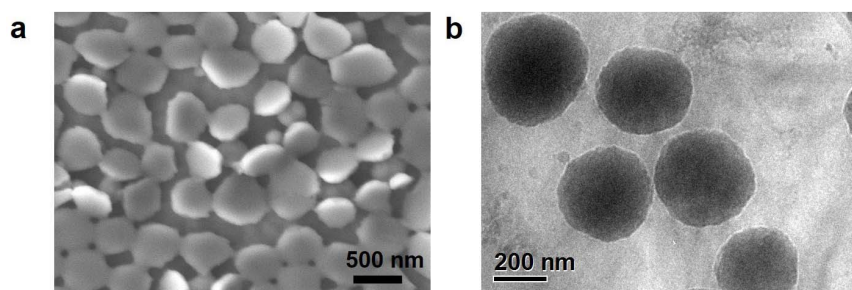


**Figure 3 | BPDI/(CB[7])<sub>2</sub> “dumbbell-shape” supra-amphiphiles self assemble into nanodiscs.** (a) SEM, (b) cryo-TEM images of BPDI/(CB[7])<sub>2</sub> self-assemblies. The concentration of BPDI is fixed at  $5.0 \times 10^{-4}$  M.

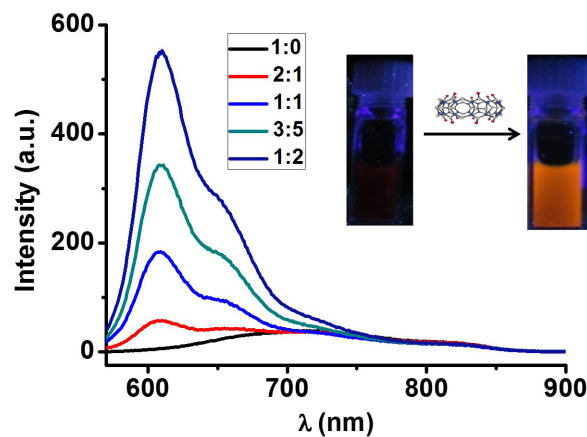


**Figure 4 | The fluorescence of the BPDI/(CB[7])<sub>2</sub> “dumbbell-shape” supra-amphiphiles is greatly increased compared with that of BPDI.** Fluorescence spectra of the BPDI-CB[7] complexes with different molar ratios. Inset: Photographs of the BPDI (left) and BPDI/(CB[7])<sub>2</sub> (right) aqueous solution upon irradiation with a 354 nm light source. The concentration of BPDI is fixed at  $5.0 \times 10^{-4}$  M.

Thus, the observed increase of absorptions should then be ascribed to the increased distance between the PDI chromophores. This speculation is further supported by <sup>1</sup>H-NMR spectroscopy. As shown in Figure 5b and Supplementary Figure S4, in the NMR spectrum for the BPDI assemblies, the signals were very weak and noisy especially at the aromatic region, indicating that the PDI aromatic rings are in the severely aggregated state. In contrast, the NMR spectrum for the BPDI/(CB[7])<sub>2</sub> supra-amphiphiles became much more clearer and the peaks got isolated with each other, thus indicating that the bulky CB[7] has prohibited the close  $\pi$ - $\pi$  stacking of the PDI chromophores in the assemblies<sup>29,46</sup>.

We were curious about whether the noncovalent method established here is also effective for the fabrication of supramolecular fluorescent solid-state thin films. A thin and solid film was prepared by drop-casting the BPDI/(CB[7])<sub>2</sub> solution onto glass slides. As shown by the fluorescence microscopy images in Figure 5c, the film emits an intense red light under illumination. By great contrast, the thin film of BPDI is non-emissive. Thus, the noncovalently fabricated “dumbbell-shape” supra-amphiphiles can provide an easy and efficient way for the fabrication of a highly fluorescent supramolecular solid-state material which are originally non-emissive due to fluorescence quenching.

**The “dumbbell-shape” supra-amphiphiles show great adaptivity.** The supramolecular approach to fabricate highly fluorescent aggregates not only has greatly decreased the number of required synthetic steps, and also allows for the construction of smart soft



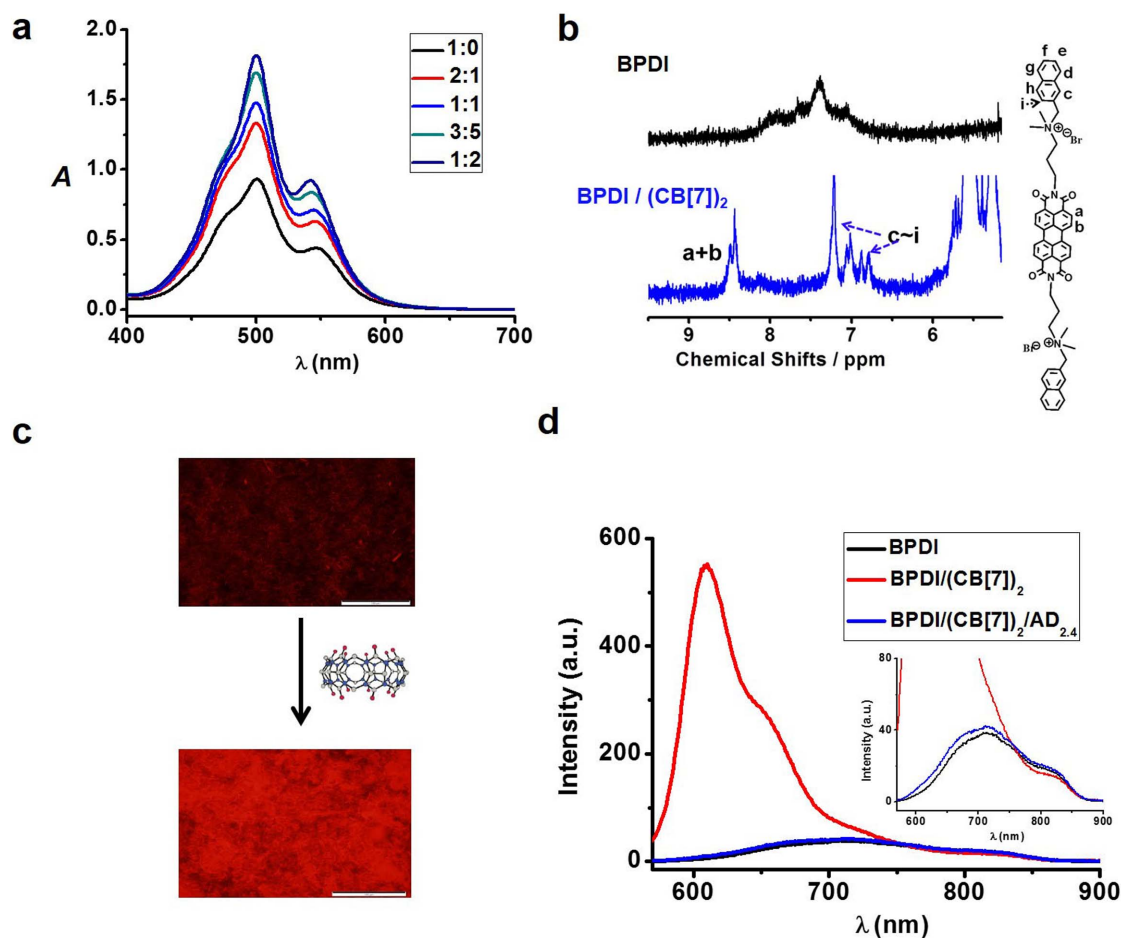


**Figure 5** | The reason for the enhanced fluorescence of the BPDI/(CB[7])<sub>2</sub> “dumbbell-shape” supra-amphiphiles and their adaptivity. (a) UV/Vis spectra of the BPDI-CB[7] complexes with different molar ratios. The molar ratio shown in the inset is defined as BPDI:CB[7]. (b)  $^1\text{H-NMR}$  spectra of BPDI (black) and BPDI/(CB[7])<sub>2</sub> (blue). The solvent is D<sub>2</sub>O. (c) Fluorescence microscopic images of BPDI (left) and BPDI/(CB[7])<sub>2</sub> (right) solid-state thin films. The samples are irradiated with a 550 nm light source. The scale bar is 110  $\mu\text{m}$ . (d) Fluorescence spectra of BPDI (black curve), BPDI/(CB[7])<sub>2</sub> (red curve) and BPDI/(CB[7])<sub>2</sub>/AD<sub>2.4</sub> (blue curve) aqueous solution. The concentration of BPDI is fixed at  $5.0 \times 10^{-4}$  M.

materials with great adaptivity, inherited from the reversible host-guest interactions. 1-Adamantanamine hydrochloride (AD), which has a stronger complexation with CB[7]<sup>25–32,40</sup>, was added into the BPDI/(CB[7])<sub>2</sub> complex solution until a molar ratio of BPDI:CB[7]:AD = 1:2:2.4 was obtained. As expected, the preferred binding of CB[7] to the AD guests can lead to the dissociation of the BPDI/(CB[7])<sub>2</sub> supra-amphiphiles. From mass spectroscopy, the peaks corresponding to the BPDI/(CB[7])<sub>2</sub> supra-amphiphiles ( $m/z = 1584.66$ ) disappear completely, whereas the peak corresponding to the AD/CB[7] complex ( $m/z = 1314.62$ ) appears (see Supplementary Figure S6a), indicating the successful dissociation of CB[7] from the “dumbbell-shape” supra-amphiphiles by the competing AD guests. DLS measurements also indicate the successful recovery from the BPDI/(CB[7])<sub>2</sub> supra-amphiphiles to BPDI amphiphiles. The assemblies with a hydrodynamic diameter of  $\sim 100$  nm formed from the supra-amphiphiles disappear, while larger aggregates with a hydrodynamic diameter of  $\sim 1000$  nm appear, which is about the same size as that formed by BPDI alone, as shown in Supplementary Figure S6b. Moreover, the morphology of the assemblies are similar to that of the BPDI alone, as indicated by the TEM images (Supplementary Figure S6c). No nanodiscs can be observed, confirming the dissociation of the supra-amphiphiles. Further, after the addition of the competitive AD, the fluorescence of the solution recovers to the initial highly quenched state, as shown in Figure 5d and Supplementary Figure S6d. The fluorescence of the

BPDI/(CB[7])<sub>2</sub>/AD<sub>2.4</sub> system is nearly the same as that of BPDI, indicating that the current system is highly reversible and adaptive.

**The adaptive supra-amphiphiles can be used as supramolecular sensor for spermine.** The highly adaptive “dumbbell-shape” supra-amphiphiles can be used as a supramolecular sensor for the fast and ultra-sensitive detection of spermine. Spermine is a biologically active amine formed by usual metabolic processes in cells and plays an important role in regulating cell growth and differentiation<sup>47,48</sup>. The detection of spermine is important because of its toxicity and its usage as tumor biomarking properties. Elevated spermine concentrations in body fluid is reported to be indicative of the presence of rapidly growing malignant tumors, and monitoring spermine in body fluid is proposed as a tool for early diagnosis and to assess the efficacy of cancer therapy<sup>49,50</sup>. However, the sensitive and selective detection of spermine is greatly hindered by its low molecular weight, low volatility and lack of chromophores. Although the spermine is currently detected using immunoassays<sup>51</sup> and chromatographic techniques<sup>47,52,53</sup>, these are time-consuming, tedious procedures, involving expensive equipment.

In our current system, considering the adaptive nature of the supra-amphiphiles and the simultaneous dramatic fluorescence change, we have explored the possibility of utilizing this system for the detection of ultra-trace amounts of spermine. Spermine can preferably bind to CB[7] due to the existence of multiple positive charges



and long alkyl chains (binding constant  $K = 2.6 \times 10^7 \text{ M}^{-1}$ )<sup>54,55</sup> (Figure 6a and Supplementary Figure S7), thus leading to the dissociation of the supra-amphiphiles and the simultaneous quenching of the fluorescence. As shown in Figure 6b, when spermine is added into the aqueous solution containing 500 nM of the “dumbbell-shape” supra-amphiphile, the fluorescence of PDI is reduced. As a control experiment, spermine could not quench the fluorescence of the BPDI alone without CB[7], further supporting the sensing mechanism as shown in Figure 6a. The extent of fluorescence quenching is then plotted against concentration of spermine, thus the working curve of the supramolecular sensor can be obtained, as shown in the inset of Figure 6c (black dots). The supramolecular sensor is very

sensitive to the concentrations of spermine even down to the range of tens of nanomolar concentrations. Only 30 nM of spermine can cause a 10% quenching of the fluorescence, which is among the most sensitive sensors for spermine to the best of our knowledge<sup>56–58</sup>. In addition, the detection range can be easily adjusted in a wide range by varying the concentration of the supra-amphiphiles. As indicated by Figure 6c, when the concentration of supra-amphiphile is fixed at 5.0  $\mu\text{M}$  (red dots), the detection limit for spermine can be adjusted to several micromolar concentrations. Further increase of the concentration of supra-amphiphile to 25  $\mu\text{M}$  allows for the sensitive detection of spermine up to  $\sim 60 \mu\text{M}$  (blue dots). The broad detection range presented here can cover the full critical concentration

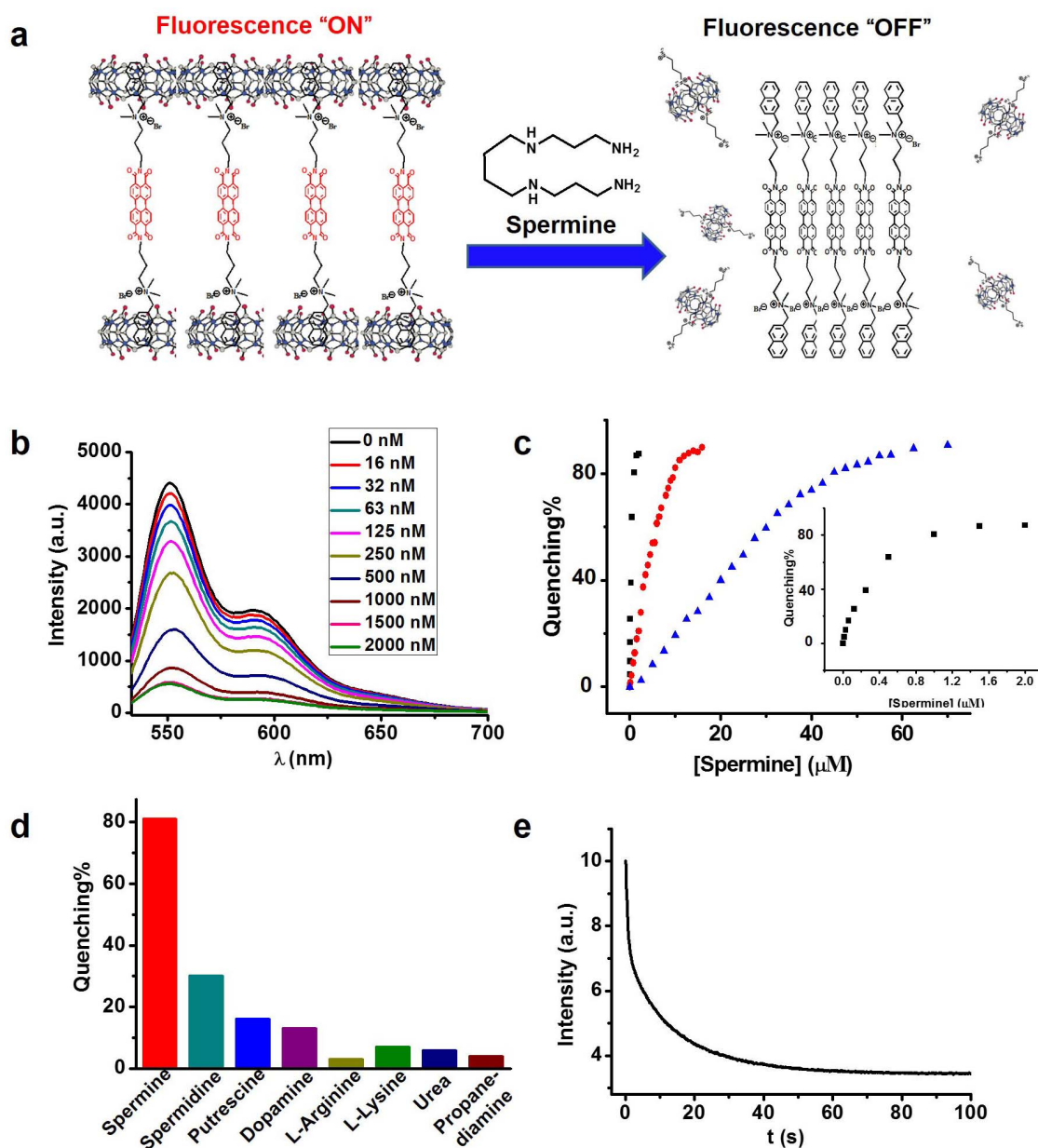


**Figure 6** | The adaptive “dumbbell-shape” supra-amphiphiles can be used as a supramolecular sensor for spermine. (a) Schematic illustration of the mechanism for sensing spermine. (b) Fluorescence spectra of the BPDl/(CB[7])<sub>2</sub> aqueous solution with different concentrations of spermine. The concentration of BPDl is fixed at 500 nM. Inset is the concentration of spermine in the solution. (c) Fluorescence emission quenching extent ( $\lambda_{\text{em}} = 553 \text{ nm}$ ) of the BPDl/(CB[7])<sub>2</sub> aqueous solution (black: 500 nM, red: 5.0  $\mu\text{M}$ , blue: 25  $\mu\text{M}$ ) with different concentrations of spermine. Inset is the enlarged curve when the concentration of BPDl/(CB[7])<sub>2</sub> supra-amphiphile is fixed at 500 nM. (d) Fluorescence emission quenching extent ( $\lambda_{\text{em}} = 553 \text{ nm}$ ) of the aqueous solution containing BPDl/(CB[7])<sub>2</sub> supra-amphiphiles (concentration: 500 nM) and different analytes (concentration: 1.0  $\mu\text{M}$ ). (e) Stopped-flow fluorescence data of BPDl/(CB[7])<sub>2</sub> supra-amphiphiles aqueous solution upon addition of spermine. The concentration of supra-amphiphiles is 5.0  $\mu\text{M}$  and that of spermine is 10.0  $\mu\text{M}$ .



range for cancer diagnosis and clinical usage<sup>59,60</sup>. Moreover, the supramolecular sensor shows good selectivity for spermine over several closely related structural analogues, such as some biological amines (spermidine, putrescine et al.) and amino acids (L-arginine, L-lysine et al.), of which the analyte-induced fluorescence quenching is small compared to that for spermine (Figure 6d). Sensing kinetics of the supramolecular sensor were also studied. The fluorescence of the supramolecular sensor can be dramatically quenched immediately at the time of spermine addition, and reaches equilibrium within  $\sim 40$  s (Figure 6e), which is the most rapid sensing system for spermine reported to date<sup>56–58</sup>, benefiting from the high adaptivity of supra-amphiphiles.

## Discussion

Upon simply adding CB[7] into the aqueous solution of BPDI, the bulky CB[7] can be noncovalently attached to the PDI chromophores, thus transforming the nonemissive nanoflowers (BPDI assemblies) into highly fluorescent nanodiscs. The reason for the enhanced fluorescence in the nanodiscs can be explained as follows: In BPDI assemblies, the fluorescence of the PDI chromophores is severely quenched due to the close contact between the PDI chromophores. However, the noncovalently attached bulky CB[7] hydrophilic heads of the supra-amphiphiles have suppressed the  $\pi$ - $\pi$  interactions and fluorescence quenching of the PDI chromophores in the aggregates, thus leading to the fabrication of highly fluorescent assemblies.

In this paper, we have explored the ability of the supra-amphiphile to act as a supramolecular sensor for spermine, an important biological amine. The supramolecular sensor shows high sensitivity and selectivity, adjustable wide detection range and rapid response rate. Although some optical spermine chemosensors have been reported recently<sup>56–58</sup>, our supramolecular sensor is unique in that it combines all the advantages in one system, which has never been achieved before and is crucial for real time biological applications.

The high performance of the current supramolecular sensor may arise from the unique molecular structures of the supra-amphiphiles. The chromophore of perylene diimide is highly hydrophobic and has a great propensity to aggregate in water even at very low concentrations of the supramolecular sensor<sup>20</sup>. Thus, the switching of the fluorescence can still occur in the presence of ultra-trace amounts of spermine with a fast response rate; The hydrophilic heads of the supra-amphiphile, CB[7], can bind specifically to the analyte based on host-guest interactions<sup>54,55</sup>, which is the reason for the high selectivity of the sensor. It is thus anticipated that, by changing the hydrophilic heads of CB[7] into other host molecules, e.g. cyclodextrins, calixarenes, supramolecular sensors for other specific analytes can be easily fabricated.

In conclusion, we have provided a novel supramolecular approach for fabricating highly emissive and smart materials using a new kind of “dumbbell-shape” supra-amphiphiles, which have greatly decreased the number of required synthetic steps and also allows for a system with switchable photophysical properties. By simply adding CB[7] into the non-emissive BPDI assemblies in water, the fluorescence of the PDI chromophores in the aggregates can be greatly increased, thus leading to the rational fabrication of highly fluorescent supramolecular materials. The supramolecular approach established here is also effective for the fabrication of highly emissive solid-state thin films. Moreover, the water-soluble “dumbbell-shape” supra-amphiphiles exhibit great adaptivity and can be used as a supramolecular sensor for the rapid detection of spermine with high sensitivity and selectivity, which is crucial for real time biological applications, for example, the early diagnosis of malignant tumors. It is anticipated that these “dumbbell-shape” supra-amphiphiles and analogues could be useful for the fabrication of new kinds of functional supramolecular smart materials.

## Methods

**Synthesis of BPDI.** The synthesis route to BPDI is depicted in Supporting Information. The purity was confirmed by <sup>1</sup>H NMR spectroscopy and electrospray ionization mass spectrometry (ESI-MS).

**Instrumentation and methods.** <sup>1</sup>H-NMR and electrospray ionization mass spectrometry (ESI-MS): The NMR spectra were obtained using a JOEL JNM-ECA400 apparatus. The ESI-MS spectra were recorded using a PE Sciex API 3000 apparatus. DLS measurements were performed using a Malvern NanoZS90 apparatus. The UV-Vis spectra were measured using a HITACHI U-3010 spectrophotometer (path length: 1.0 mm). The fluorescence spectra were measured using a HITACHI F-7000 apparatus. For the experiment in Figure 4, the excitation wavelength is 550 nm, slit: 10.0 nm, scanning rate: 240 nm/min. For the supramolecular sensor experiments (Figure 6), a pH 3 aqueous solution is used for all the experiments. The excitation wavelength is 510 nm for the all the fluorescence measurements.

**Stopped-flow fluorescence experiments.** Time-dependent fluorescence tests were carried out by using the fluorescent mode on a Chirascan spectrometer (Applied Photophysics, UK) equipped with a stopped-flow accessory. The optical pathlength was set to 10 mm. The excitation wavelength was fixed at 510 nm and the emission signal, passing through a 540 nm filter, was recorded by a fluorescence detector.

**Isothermal titration microcalorimetry.** All measurements were performed using a TAM 2277-201 microcalorimetric system (Thermometric AB, Järfälla, Sweden) with a stainless steel sample cell of 1 mL. The sample cell was initially loaded with 0.7 mL of buffer or 0.1 mL host solution. The guest solution was injected into the sample cell via a 500  $\mu$ L Hamilton syringe controlled by a 612 Thermometric Lund pump. A series of injections were made until the desired concentration range had been covered. The system was stirred at 60 rpm with a gold propeller. The observed enthalpy ( $\Delta H_{obs}$ ) was obtained by integration over the peak for each injection in the plot of heat flow P against time t. The dilution heats of the guest were subtracted from the heats of guest-host binding experiments. By fitting the observed enthalpy curves plotted against the molar ratio of guest to host, the binding constants (K<sub>b</sub>) and the enthalpy changes ( $\Delta H$ ) of binding were derived. All of the measurements were conducted at  $298.15 \pm 0.01$  K.

**TEM.** For TEM observations, a JEMO 2010 electron microscope was used operating at an acceleration voltage of 120 kV. The samples were prepared by drop-coating the aqueous solution on a carbon-coated copper grid and were then negatively stained with a uranyl acetate or phosphotungstic acid solution.

**Cryo-TEM.** Samples were prepared in a controlled environment vitrification system (CEVS) at 28°C. The vitrified samples were stored in liquid nitrogen until they were transferred to a cryogenic sample holder (Gatan 626) and examined by a JEM2200FS TEM (200 kV) at about  $-174^\circ\text{C}$ .

**SEM.** A JEOL JSM-7401F field-emission scanning electron microscope was used operating at 3.0 kV. The sample was prepared by drop-coating the aqueous solution on a Si substrate and then dried under moist conditions. The sample was directly mounted onto the microscope for imaging.

**Fluorescence microscopy.** Fluorescence images were recorded on an Olympus BX 51 apparatus upon irradiation with a 550 nm light source. In the experiments, the samples were prepared by drop-coating the aqueous solution onto a glass slide and then drying in air. The same exposure time (50 ms) was adopted for all samples to ensure the same intensity of excitation.

- Ajayaghosh, A., Carol, P. & Sreejith, S. A ratiometric fluorescence probe for selective visual sensing of  $\text{Zn}^{2+}$ . *J. Am. Chem. Soc.* **127**, 14962–14963 (2005).
- Basabe-Desmonts, L., Reinhoudt, D. N. & Crego-Calama, M. Design of fluorescent materials for chemical sensing. *Chem. Soc. Rev.* **36**, 993–1017 (2007).
- Qian, Y. *et al.* Selective fluorescent probes for live-cell monitoring of sulphide. *Nat. Commun.* **2**: 495 doi: 10.1038/ncomms1506 (2011).
- Ehli, C. *et al.* Manipulating single-wall carbon nanotubes by chemical doping and charge transfer with perylene dyes. *Nat. Chem.* **1**, 243–249 (2009).
- Huang, Y., Kuang, J., Hu, W., Wei, Z. & Faul, C. F. J. Modulating helicity through amphiphilicity—tuning supramolecular interactions for the controlled assembly of perylenes. *Chem. Commun.* **47**, 5554–5556 (2011).
- Krieg, E. *et al.* A recyclable supramolecular membrane for size-selective separation of nanoparticles. *Nat. Nanotechnol.* **6**, 141–146 (2011).
- O’neil, M. P. *et al.* Picosecond optical switching based on biphotonic excitation of an electron donor-acceptor-donor molecule. *Science* **257**, 63–65 (1992).
- Yang, Q. *et al.* Detection and differential diagnosis of colon cancer by a cumulative analysis of promoter methylation. *Nat. Commun.* **3**: 1206 doi: 10.1038/ncomms2209 (2012).
- Zlezer, M., Scurr, D. J., Alexander, M. R. & Ulijn, R. V. Development and validation of a fluorescence method to follow the build-up of short peptide sequences on solid 2d surfaces. *ACS Appl. Mater. Interfaces* **4**, 53–58 (2012).
- Yagai, S. *et al.* Supramolecularly engineered perylene bisimide assemblies exhibiting thermal transition from columnar to multilamellar structures. *J. Am. Chem. Soc.* **134**, 7983–7994 (2012).





11. Würthner, F. Perylene bisimide dyes as versatile building blocks for functional supramolecular architectures. *Chem. Commun.* **14**, 1564–1579 (2004).
12. Zhang, X., Rehm, S., Safont-Sempere, M. M. & Würthner, F. Vesicular perylene dye nanocapsules as supramolecular fluorescent pH sensor systems. *Nat. Chem.* **1**, 623–629 (2009).
13. Avinash, M. B. & Govindaraju, T. Amino acid derivatized arylenediimides: a versatile modular approach for functional molecular materials. *Adv. Mater.* **24**, 3905–3922 (2012).
14. Hoeben, F. J. M. *et al.* About supramolecular assemblies of  $\pi$ -conjugated systems. *Chem. Rev.* **105**, 1491–1546 (2005).
15. Wang, B. & Yu, C. Fluorescence turn-on detection of a protein through the reduced aggregation of a perylene probe. *Angew. Chem. Int. Ed.* **49**, 1485–1488 (2010).
16. Dössel, L. F. *et al.* Synthesis and Controlled self-assembly of covalently linked hexa-peri-hexabenzocoronene/peryrene diimide dyads as models to study fundamental energy and electron transfer processes. *J. Am. Chem. Soc.* **134**, 5876–5886 (2012).
17. Liu, Y. *et al.* Supramolecular assembly of perylene bisimide with  $\beta$ -cyclodextrin grafts as a solid-state fluorescence sensor for vapor detection. *Adv. Funct. Mater.* **19**, 2230–2235 (2009).
18. Heek, T. *et al.* Highly fluorescent water-soluble polyglycerol-dendronized perylene bisimide dyes. *Chem. Commun.* **46**, 1884–1886 (2010).
19. Yang, S. K. *et al.* Monovalent, clickable, uncharged, water-soluble perylenebisimide-cored dendrimers for target-specific fluorescent biolabeling. *J. Am. Chem. Soc.* **133**, 9964–9967 (2011).
20. Görl, D., Zhang, X. & Würthner, F. Molecular assemblies of perylene bisimide dyes in water. *Angew. Chem. Int. Ed.* **51**, 6328–6348 (2012).
21. Kaiser, T. E., Wang, H., Stepanenko, V. & Würthner, F. Supramolecular construction of fluorescent J-aggregates based on hydrogen-bonded perylene dyes. *Angew. Chem. Int. Ed.* **46**, 5541–5544 (2007).
22. Kumar, M. & George, S. J. Green fluorescent organic nanoparticles by self-assembly induced enhanced emission of a naphthalene diimide bolaamphiphile. *Nanoscale* **3**, 2130–2133 (2011).
23. An, B. K. *et al.* Enhanced emission and its switching in fluorescent organic nanoparticles. *J. Am. Chem. Soc.* **124**, 14410–14415 (2002).
24. Luo, J. D. *et al.* Aggregation-induced emission of 1-methyl-1,2,3,4,5-pentaphenylsilole. *Chem. Commun.* 1740–1741 (2001).
25. Kim, K. *et al.* Functionalized cucurbiturils and their applications. *Chem. Soc. Rev.* **36**, 267–279 (2007).
26. Liu, S. M. *et al.* The cucurbit[n]uril family: prime components for self-sorting systems. *J. Am. Chem. Soc.* **127**, 15959–15967 (2005).
27. Casado, A. G., Jonkheijm, P. & Huskens, J. Recognition properties of cucurbit[7]uril self-assembled monolayers studied with force spectroscopy. *Langmuir* **27**, 11508–11513 (2011).
28. Das, D. & Scherman, O. A. Cucurbituril: at the interface of small molecule host-guest chemistry and dynamic aggregates. *Isr. J. Chem.* **51**, 537–550 (2011).
29. Biedermann, F. *et al.* Strongly fluorescent, switchable perylene bis(diimide) host-guest complexes with cucurbit[8]uril in water. *Angew. Chem. Int. Ed.* **51**, 7739–7743 (2012).
30. Gadde, S. *et al.* Control of H- and J-aggregate formation via host-guest complexation using cucurbituril hosts. *J. Am. Chem. Soc.* **130**, 17114–17119 (2008).
31. Dsouza, R. N., Pischel, U. & Nau, W. M. Fluorescent dyes and their supramolecular host/guest complexes with macrocycles in aqueous solution. *Chem. Rev.* **111**, 7941–7980 (2011).
32. Hennig, A., Bakirci, H. & Nau, W. M. Label-free continuous enzyme assays with macrocycle-fluorescent dye complexes. *Nat. Methods* **4**, 629–632 (2007).
33. Kim, H. J. *et al.* Selective inclusion of a hetero-guest pair in a molecular host: formation of stable charge-transfer complexes in cucurbit[8]uril. *Angew. Chem. Int. Ed.* **40**, 1526–1529 (2001).
34. Liu, Y. L. *et al.* Water-Soluble Supramolecular Polymerization Driven by Multiple Host-Stabilized Charge-Transfer Interactions. *Angew. Chem. Int. Ed.* **49**, 6576–6579 (2010).
35. Zhang, X. & Wang, C. Supramolecular amphiphiles. *Chem. Soc. Rev.* **40**, 94–101 (2011).
36. Wang, C., Wang, Z. Q. & Zhang, X. Amphiphilic building blocks for self-assembly: from amphiphiles to supra-amphiphiles. *Acc. Chem. Res.* **45**, 608–618 (2012).
37. Liu, K., Wang, C., Li, Z. B. & Zhang, X. Superamphiphiles based on directional charge-transfer interactions: from supramolecular engineering to well-defined nanostructures. *Angew. Chem. Int. Ed.* **50**, 4952–4956 (2011).
38. Tao, W. *et al.* A linear-hyperbranched supramolecular amphiphile and its self-assembly into vesicles with great ductility. *J. Am. Chem. Soc.* **134**, 762–764 (2012).
39. Guo, D. S. *et al.* Cholinesterase-responsive supramolecular vesicle. *J. Am. Chem. Soc.* **134**, 10244–10250 (2012).
40. Zeng, Y. *et al.* Enhancement of energy utilization in light-harvesting dendrimers by the pseudorotaxane formation at periphery. *J. Am. Chem. Soc.* **131**, 9100–9106 (2009).
41. Seibt, J. *et al.* Vibronic transitions and quantum dynamics in molecular oligomers: a theoretical analysis with an application to aggregates of perylene bisimides. *J. Phys. Chem. A* **113**, 13475–13482 (2009).
42. Lokey, R. S. & Iverson, B. L. Synthetic molecules that fold into a pleated secondary structure in solution. *Nature* **375**, 303–305 (1995).
43. Cantor, R. C. & Schimmel, P. R. *Biophysical Chemistry Part II*, Freeman, New York, 1980, pp. 390.
44. Chen, Z. *et al.* Photoluminescence and Conductivity of Self-Assembled  $\pi$ - $\pi$  Stacks of Perylene Bisimide Dyes. *Chem. Eur. J.* **13**, 436–439 (2007).
45. Hädicke, E. *et al.* Structures of eleven perylene-3,4:9,10-bis(dicarboximide) pigments. *Acta Crystallogr., Sect. C* **42**, 189–195 (1986).
46. Zhao, N. *et al.* Binding studies on CB[6] with a series of 1-alkyl-3-methylimidazolium ionic liquids in an aqueous system. *Chem. Asian J.* **5**, 530–537 (2010).
47. Bachrach, U. Polyamines and cancer: minireview article. *Amino Acids* **26**, 307–309 (2004).
48. Durie, B. G. M., Salmon, S. E. & Russell, D. H. Polyamines as markers of response and disease activity in cancer chemotherapy. *Cancer Res.* **37**, 214–221 (1977).
49. Russel, D. H. Increased polyamine concentrations in the urine of human cancer patients. *Nature* **233**, 144–145 (1971).
50. Russel, D. H. Clinical relevance of polyamines as biochemical markers of tumor kinetics. *Clin. Chem.* **23**, 22–27 (1977).
51. Kawakita, M. & Hiramatsu, K. Diacetylated derivatives of spermine and spermidine as novel promising tumor markers. *J. Biochem.* **139**, 315–322 (2006).
52. Byun, J. A. *et al.* Serum polyamines in pre- and post-operative patients with breast cancer corrected by menopausal status. *Cancer Lett.* **273**, 300–304 (2009).
53. Paik, M. J. *et al.* Altered urinary polyamine patterns of cancer patients under acupuncture therapy. *Amino Acids* **37**, 407–413 (2009).
54. Mock, W. L. & Shih, N. Y. Structure and selectivity in host-guest complexes of cucurbituril. *J. Org. Chem.* **51**, 4440–4446 (1986).
55. Carvalho, C. D. P. C. Supramolecular biomimetic binding of the DNA-dye Hoechst 33258 by a synthetic macrocycle. Master Dissertation, the University of the Algarve (2010).
56. Kösterli, Z. & Severin, K. Fluorescence sensing of spermine with a frustrated amphiphile. *Chem. Commun.* **48**, 5841–5843 (2012).
57. Ikeda, M. *et al.* Montmorillonite–supramolecular hydrogel hybrid for fluorocolorimetric sensing of polyamines. *J. Am. Chem. Soc.* **133**, 1670–1673 (2011).
58. Satrijo, A. & Swager, T. M. Anthryl-doped conjugated polyelectrolytes as aggregation-based sensors for nonquenching multicationic analytes. *J. Am. Chem. Soc.* **129**, 16020–16028 (2007).
59. Uehara, N. *et al.* Elevated contents of spermidine and spermine in the erythrocytes of cancer patients. *Cancer* **45**, 108–111 (1980).
60. Marton, L. J., Russell, D. H. & Levy, C. C. Measurement of putrescine, spermidine, and spermine in physiological fluids by use of an amino acid analyzer. *Clin. Chem.* **19**, 923–926 (1973).

## Acknowledgements

This work was financially supported by the National Basic Research Program (2013CB834502), the NSFC (50973051, 20974059), NSFC-DFG joint grant (TRR 61), the Foundation for Innovative Research Groups of the NSFC (21121004), as well as by the Tsinghua University Initiative Scientific Research Program (2009THZ02230). Thanks to Dr. Huaping Xu, Dr. Juan Qiao, Prof. Dongsheng Liu and Miss Chun Chen for their helpful discussions.

## Author contributions


K. L. and X. Z. conceived and designed the experiments; K. L., Y. X. Y. and Y. T. K., performed the experiments; Y. L. and Z. B. L. performed the cryo-TEM experiments; Y. C. H. and Y. L. W. performed the ITC experiments and analysed the ITC data; K. L. and X. Z. wrote the paper.

## Additional information

Supplementary information accompanies this paper at <http://www.nature.com/scientificreports>

**Competing financial interests:** The authors declare no competing financial interests.

**How to cite this article:** Liu, K. *et al.* A supramolecular approach to fabricate highly emissive smart materials. *Sci. Rep.* **3**, 2372; DOI:10.1038/srep02372 (2013).

 This work is licensed under a Creative Commons Attribution-NonCommercial-NoDerivs 3.0 Unported license. To view a copy of this license, visit <http://creativecommons.org/licenses/by-nc-nd/3.0>